

Classical and Quantum Analysis of Repulsive Singularities in Four Dimensional Extended Supergravity

I. Gaida, H. R. Hollmann¹ and J. M. Stewart²

Department of Applied Mathematics and Theoretical Physics,
Silver Street, Cambridge CB3 9EW, England

Abstract

Non-minimal repulsive singularities (“repulsons”) in extended supergravity theories are investigated. The short distance antigravity properties of the repulsons are tested at the classical and the quantum level by a scalar test-particle. Using a partial wave expansion it is shown that the particle gets totally reflected at the origin. A high frequency incoming particle undergoes a phase shift of $\frac{\pi}{2}$. However, the phase shift for a low-frequency particle depends upon the physical data of the repulson. The curvature singularity at a finite distance r_h turns out to be transparent for the scalar test-particle and the coordinate singularity at the origin serves as a repulsive barrier at which particles bounce off.

Keywords: Supergravity, Physics of Black Holes, Quantum Computation.

PACS: 04.70, 04.65, 03.67.L

¹e-mail: H.Hollmann@damtp.cam.ac.uk

²e-mail: J.M.Stewart@damtp.cam.ac.uk

1 Introduction

In the last years there has been a lot of progress in understanding black hole physics in supergravity and string theory in $N > 1$ supersymmetric vacua (for recent reviews see [1]). A lot of these black hole solutions can be interpreted as certain (non-singular) p -brane solutions, too [2]. This opens the possibility to obtain a microscopic understanding of the macroscopic Bekenstein–Hawking entropy [3]. Another interesting point in this context is the appearance of massless black holes at particular points in moduli space giving rise to gauge symmetry enhancement or supersymmetry enhancement [4, 5]. However, in [4, 6, 7, 8, 9] it also has been shown that not only attractive singularities (black holes) are stable BPS solutions of these supersymmetric vacua, but that repulsive naked singularities (“repulsons”) appear too. Thus, repulsons are non-perturbative manifestations of antigravity effects in supersymmetric vacua. With antigravity we mean in this context the property of these solutions to reflect particles with a given mass or angular momentum ([6]). It has known for a long time that antigravity effects occur at the perturbative level in extended supergravity [10].

It has been pointed out in [9] that repulsons, sometimes also called “white holes”, are as generic in moduli space as their “dual” attractive singularities (black holes). In addition a “minimal” repulson background has been analysed in [6, 9] using a scalar test-particle and expanding the corresponding wave function in partial waves. It has been shown that at the classical level no massive scalar test-particle can reach the “outer” curvature singularity at $r_h > 0$. Moreover, at the quantum level the “inner” singularity at the origin is reflecting, but the “outer” singularity is transparent. In this context it has been assumed that the scalar test-particle can tunnel through the “outer” curvature singularity. In addition it has been “suggested” that for $r > r_h$ space-time is Minkowskian and for $r < r_h$ space-time is Euclidean. In addition it is important to note that the Dirac quantization condition plays a non-trivial role in these considerations [9].

It is interesting that repulson solutions are supersymmetric extensions of the Reissner–Weyl solution [11], which served as an effective model for the electron in the 50’s. Repulsons have the “realistic” physical property that they are gravitational attractive at large distances and gravitational repulsive at short distances. Hence, repulsons yield the usual Newtonian gravity at large distances, but at short distances, i.e. at the order of the Planck length 10^{-33} cm, for example, Newtonian gravity is not valid.

The main purpose of this article is to extend the analysis of [6, 9] in order to study “non-minimal” repulson backgrounds and the associated antigravity effects. Although we will restrict ourselves to a particular supersymmetric model and particular charge configurations, most of our results are quite general.

The article is organized as follows: To make the article sufficiently self-contained we start with a short outline of the static solutions of the $N = 2$ bosonic

sector of extended supergravity in four dimensions. In particular we introduce the metric background which we call a “repulson” in the following. In the next section we define the specific repulson models we are investigating and outline some properties of the space–time they form. The remaining part of the paper is dedicated to the properties of these repulsive singularities: we model the repulson by a family of potentials and consider a test–particle initially moving towards the singularity at the origin. The classical analysis (section 4) tells that the particle is reflected at a distance r_{min} away from the origin. r_{min} is actually bigger than r_h , the position of the curvature singularity of the underlying repulson space–time. By a Hamilton–Jacobi analysis the time the particle needs to get from a position r_1 to r_2 and the trajectory itself are calculated. In section 5 a quantum mechanical analysis is presented. It is defined by a Klein–Gordon equation on the background of the repulson. The geometry is spherically symmetric, so that we get an ordinary differential equation for the Fourier modes. For special choices of the parameters in the repulson model the Klein Gordon equation can be solved analytically. For other sets of data we present a numerical solution and in addition some semi–classical results in terms of a matched asymptotic expansion. In the next section we compare the numerical data with the data given by the matched asymptotic expansion, which has the nice feature that it provides the relation between the amplitude of the ingoing and the outgoing mode and the phase shift between them. That is, the scattering data can be read off. The asymptotic expansion of the analytical solution provides us with some deeper insight of the scattering behaviour even for an incoming particle with a low frequency. We finish the paper by summarizing what has been worked out, by an outline of the future lines of investigation and by some speculations what the results may imply physically.

2 Static Solutions of $N = 2$ Supergravity

The repulsons we are investigating are solutions of the bosonic sector of $N = 2$ supergravity in four dimensions. In this section we briefly outline [4, 12, 13], how these solutions are obtained.

The action of the bosonic truncation of $N = 2$ supergravity in four dimensions includes a gravitational, vector and hypermultiplets. The hypermultiplets are assumed to be constant. The complex scalars of the vector multiplets form a sigma model the target space of which is special Kähler. That is, the real Kähler potential K , which defines the sigma model metric, is entirely determined by a holomorphic and homogeneous function, the prepotential \mathcal{F} . All the fields of the theory can be expressed in terms of the vector $\Omega = (X^I, \mathcal{F}_I)$, where $I = 0, \dots, N_v$ counts the number of the physical vectors and N_v the scalars. The components of Ω are the holomorphic sections of a line bundle over the moduli space. With \mathcal{F}_I we denote $\mathcal{F}_I = \frac{\partial \mathcal{F}(X)}{\partial X^I}$. In order to enforce the configuration to

be supersymmetric the so called stabilization equations [8] have to be satisfied

$$i(X^I - \bar{X}^I) = H^I(x^\mu), \quad i(\mathcal{F}_I - \bar{\mathcal{F}}_I) = H_I(x^\mu).$$

Because of the equations of motion and the Bianchi identities, the functions H^I and H_I are harmonic. To derive explicit solutions in general and the repulson solution in particular, the prepotential and the harmonic functions have to be specified. The repulsons arise in the context of a model with prepotential

$$\mathcal{F}(S, T, U) = -STU, \quad \text{with} \quad (S, T, U) = -i z^{1,2,3}.$$

The $z^{1,2,3}$ are defined by so called special coordinates $X^0(z) = 1$, $X^A(z) = z^A$, $A = 1, \dots, N_v$. In string theory this prepotential corresponds to the classical heterotic STU -model with constant hypermultiplets. The microscopic interpretation, the higher order curvature corrections, the near extremal approximation, and the effect of quantum corrections of this class of $N = 2$ models has been studied extensively in [5, 14, 15].

For simplicity we take all moduli to be axion-free, that is purely imaginary. Solving the stabilisation equations with respect to these constraints yields

$$S, T, U = \frac{H^{1,2,3}}{2X^0}, \quad X^0 = \frac{1}{2} \sqrt{-D/H_0} \quad (1)$$

with $D = H^1 H^2 H^3$. The harmonic functions are given by the constants h , the electric and magnetic charges q and p , respectively

$$H^I(r) = h^I + \frac{p^I}{r}, \quad H_I(r) = h_I + \frac{q_I}{r}.$$

The charges satisfy the Dirac quantisation condition $p q = 2\pi n$, $n \in \mathbb{Z}$. If we restrict ourselves to static spherically symmetric solutions only, the most general ansatz for the metric is

$$ds^2 = -\frac{1}{F(r)} dt^2 + F(r) (dr^2 + r^2 d\Omega_2^2). \quad (2)$$

The metric function $F(r)$ is given by

$$F = e^{-K} = i(\bar{X}^A \mathcal{F}_A - X^A \mathcal{F}_A), \quad A = 1, 2, 3.$$

Here $F^2(r)$ reads

$$F^2(r) = -4 H_0 D = \sum_{n=0}^4 \frac{\alpha_n}{r^n}.$$

It is possible to choose the parameters of the harmonic functions such that the solutions correspond to *repulsive* singular supersymmetric states [7]. It is straightforward to see whether these solutions are gravitational attractive or repulsive.

q_0	p^1	p^2	p^3	(anti-)gravity	#
+	+	+	+	attractive	1
-	+	+	+	repulsive	4
-	-	+	+	attractive	6
-	-	-	+	repulsive	4
-	-	-	-	attractive	1

Here we denote $p, q > 0$ (< 0) by $+$ ($-$) and include possible permutations when denoting the number # of repulsive and attractive solutions. Note that any positive (negative) charge appearing in the solution can be interpreted as an (anti-)brane [8, 9]. Moreover, the solution with four antibranes, i.e. all charges are negative, yields a *negative* ADM mass.

3 Scalar Particles in the Background of a Repulson

In the following the repulson singularities are investigated. For that we follow the motion of a test-particle moving in the metric background produced by the repulson. The repulson gets effectively modelled by a family of potentials, defined by the metric function $F^2(r)$. The parameters $\alpha_1, \dots, \alpha_4$ determine the shape of the potentials.

In order to obtain flat space-time at spatial infinity α_0 is chosen to be equal to 1. In addition we shall consider charge configurations with positive ADM mass, i.e. $\alpha_1 > 0$. For a repulson configuration the coefficient α_2 in the metric function is negative. The short distance behaviour is dominated by the $\frac{1}{r^4}$ -term in the metric function. Therefore the solution is gravitationally attractive at short distances if $\alpha_4 > 0$ and gravitationally repulsive if $\alpha_4 < 0$. We restrict ourselves to the case $\alpha_4 < 0$ only. We put in a further simplification: α_3 is defined by

$$\alpha_1^3 + 8\alpha_3 - 4\alpha_1\alpha_2 = 0 \quad (3)$$

With these restrictions on $\alpha_1, \dots, \alpha_4$ the function $F^2(r)$ has the generic form illustrated in **figure 1a** and **figure 1b**. **Figure 1a** shows the shape of $F^2(r)$ for $\alpha_3 = \alpha_4 = 0$. The parameters (α_1, α_2) are chosen to be $(10.0, -10.0)$, $(11.0, -9.0)$, $(12.0, -8.0)$ and $(13.0, -7.0)$ with lines of increasing thickness. In **figure 1b** the shape of the metric function is plotted for some values of α_i , with $\alpha_3, \alpha_4 \neq 0$. The triples of parameters (increasing thickness of the lines) are $(\alpha_1, \alpha_2, \alpha_4) = (4.0, -1.0, -4.0)$, $(3.0, -1.0, -3.0)$, $(2.0, -1.0, -2.0)$ and $(1.0, -1.0, -1.0)$.

The coefficients which appear in the metric function are related to the physical parameters. $\alpha_1 = 4M \geq 0$, where M denotes the ADM mass, and $\alpha_2 = -4Z^2 < 0$. Z is the central charge of the configuration. With (3) we find $\alpha_3 = -8M(M^2 + Z^2) < 0$ and α_4 is a free parameter, for a repulson configuration chosen to be less than zero.

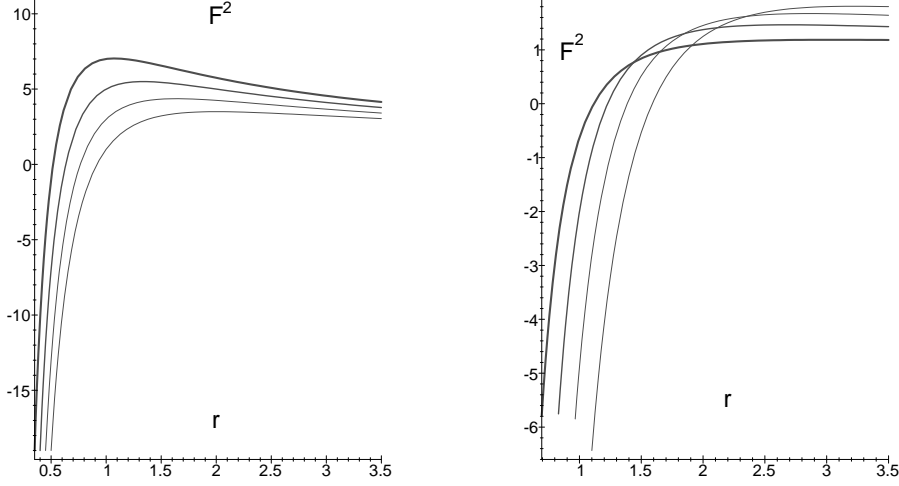


figure 1a: shape of the metric function $F^2(r)$ for $\alpha_3 = \alpha_4 = 0$ **figure 1b:** shape of the metric function $F^2(r)$ for $\alpha_3, \alpha_4 \neq 0$

$F^2(r)$ has exactly one zero at a distance $r_h > 0$, which is given by

$$r_h = \sqrt{\frac{\alpha_1^2}{16} + v_+} - \frac{\alpha_1}{4} \quad (4)$$

with

$$v_+ = -\frac{1}{2} \left(\alpha_2 - \frac{\alpha_1^2}{4} \right) + \sqrt{\frac{1}{4} \left(\alpha_2 - \frac{\alpha_1^2}{4} \right)^2 - \alpha_4},$$

if α_3 and α_4 are not simultaneously equal to zero. In terms of the physical data r_h reads

$$r_h = \sqrt{M^2 + v_+} - M \quad (5)$$

with

$$v_+ = 2(Z^2 + M^2) + \sqrt{4(Z^2 + M^2)^2 - \alpha_4}.$$

If α_3 and α_4 both vanish, the position of the zero is given by

$$r_h = \sqrt{\frac{\alpha_1^2}{4} - \alpha_2} - \frac{\alpha_1}{2} = 2(\sqrt{M^2 + Z^2} - M). \quad (6)$$

At $r = r_h$ the metric changes its signature. For $r > r_h$ is Lorentzian with the line element given by (2). As $r \rightarrow \infty$ the space-time is asymptotically Minkowskian and Schwarzschild. The Ricci scalar in this region is given by

$$R = -\frac{F''}{F^2} + \frac{1}{2} \frac{F'^2}{F^3} - \frac{2}{r} F' F^2. \quad (7)$$

Approaching r_h from above a curvature singularity is detected. In the region $0 \leq r \leq r_h$ the line element becomes Euclidean

$$ds^2 = \frac{1}{|F|} dt^2 + |F| (dr^2 + r^2 d\Omega^2). \quad (8)$$

The Ricci scalar is again given by the expression (7). We find a curvature singularity when approaching r_h from below. At $r = 0$ all the curvature invariants remain finite. It is a coordinate singularity.

4 Classical Analysis

In the classical limit, that is in the limit of large r , the Newtonian potential $\Phi(r)$ is given by

$$\Phi(r) = -\frac{1}{2} (g_{tt} + 1) = -\frac{M}{r} + \frac{Z^2}{r^2}. \quad (9)$$

The corresponding strength of the gravitational field $\Phi' = \frac{M}{r^2} - \frac{2Z^2}{r^3}$ is gravitational attractive at large distances ($r > r_c$) and gravitational repulsive for $r < r_c$. The critical distance where gravitational repulsion and attraction yield a vanishing net force is given by $r_c = 2Z^2/M$. For the classical limit still to be valid at r_c we derive a constraint on the central charge Z and the ADM mass M . We got the Newtonian potential with the requirement $|\frac{4M}{r} - \frac{4Z^2}{r^2}| < 1$. This must hold at $r = r_c$ in particular, and it follows $Z^2 > M^2$. For massless repulsons the Newtonian potential is always repulsive.

To consider the motion of a classical scalar test-particle we choose a suitable plane with e.g., $\theta = \pi/2$. The corresponding trajectory of the test-particle of mass m in this plane can be determined using Hamilton–Jacobi theory (see e.g., [6, 16]). In the classical limit for the repulson background the Hamilton–Jacobi equation

$$g^{\mu\nu} \frac{\partial\Gamma}{\partial x^\mu} \frac{\partial\Gamma}{\partial x^\nu} + m^2 = 0 \quad (10)$$

becomes

$$F \left(\frac{\partial\Gamma}{\partial t} \right)^2 - \frac{1}{F} \left(\frac{\partial\Gamma}{\partial r} \right)^2 - \frac{1}{r^2 F} \left(\frac{\partial\Gamma}{\partial\phi} \right)^2 - m^2 = 0. \quad (11)$$

By the general procedure for solving the Hamilton–Jacobi equation we take Γ to be of the form

$$\Gamma = -Et + L\phi + \Gamma_r(r), \quad (12)$$

with energy E and angular momentum L . This yields

$$\Gamma_r(r) = \int dr \sqrt{E^2 F^2 - \frac{L^2}{r^2} - m^2 F}. \quad (13)$$

Thus, from $\frac{\partial \Gamma}{\partial E} = 0$ it follows that a test-particle takes the following time to move from r_1 to r_2

$$t = E \int_{r_1}^{r_2} dr \frac{F^2}{\sqrt{E^2 F^2 - \frac{L^2}{r^2} - m^2 F}} \quad (14)$$

For $L = 0$ a massive test-particle becomes reflected by the repulson at

$$r_{min} = \frac{2}{\epsilon} \left(\sqrt{M^2 + \epsilon Z^2} - M \right) > r_h, \quad \epsilon = 1 - \frac{m^4}{E^4}. \quad (15)$$

Moreover, for $L \neq 0$ a massless test-particle becomes reflected by the repulson at

$$r_{min} = 2 \left(\sqrt{M^2 + Z^2 + \frac{L^2}{4E^2}} - M \right) > r_h. \quad (16)$$

The trajectory itself is determined by $\frac{\partial \Gamma}{\partial L} = 0$, i.e.

$$\phi = \int_{r_1}^{r_2} dr \frac{-L}{r^2 \sqrt{E^2 F^2 - \frac{L^2}{r^2} - m^2 F}}. \quad (17)$$

5 Quantum Mechanical Analysis

For the quantum mechanical analysis we consider a massless scalar test-particle with wave function $\tilde{\psi}$ satisfying the Klein-Gordon equation in the background of the repulson:

$$\partial_\mu \left(\sqrt{-g} g^{\mu\nu} \partial_\nu \tilde{\psi} \right) = 0. \quad (18)$$

Writing $\tilde{\psi} = \Psi(t, r) Y_{lm}(\theta, \phi)$ we obtain the same equation with the metric in either the Lorentzian (2) or the Euclidean region (8)

$$\Delta \Psi - \nu |F^2| \Psi_{tt} = 0, \quad (19)$$

where Δ is the flat space Laplace operator in spherical coordinates

$$\Delta = \partial_r^2 + \frac{2}{r} \partial_r - \frac{l(l+1)}{r^2}, \quad (20)$$

and ν is 1 for $r \geq r_h$ and -1 for $r < r_h$. Since (19) is a linear partial differential equation with t -independent coefficients we may perform a Fourier transform with respect to t , that is $\Psi = e^{-i\omega t} \psi(r)$, to obtain

$$\Delta \psi + \nu \omega^2 |F^2| \psi = 0. \quad (21)$$

This is a Schrödinger equation

$$\Delta_r \psi + (E - V(r)) \psi = 0, \quad (22)$$

with

$$\begin{aligned}
E &= \omega^2, \\
V(r) &= -\left(\frac{c_1}{r} + \frac{c_2}{r^2} + \frac{c_3}{r^3} + \frac{c_4}{r^4}\right), \\
\Delta_r &= \partial_r^2 + \frac{2}{r} \partial_r.
\end{aligned} \tag{23}$$

The coefficients in terms of the physical data are given by

$$c_1 = 4M\omega^2, \quad c_2 = -4Z^2\omega^2 - l(l+1), \quad c_3 = -8M\omega^2(Z^2 + M^2), \quad c_4 = \alpha_4\omega^2.$$

For $l = 0$ the potential is, up to a factor $-\omega^2$, equal to the metric function F^2 , so that the shape of the potential can be read off **figure 1a** and **figure 1b**, respectively. Let us first study the special situation $\alpha_3 = \alpha_4 = 0$ [9]. In this case the differential equations (22) simplify to

$$\Delta_r \psi + (E - V(r)) \psi = 0, \tag{24}$$

with

$$\begin{aligned}
E &= \omega^2 \\
V(r) &= -\left(\frac{c_1}{r} + \frac{c_2}{r^2}\right).
\end{aligned} \tag{25}$$

Here we have taken into account that at the border of the Euclidean and Minkowski region of the metric not only ν but $F^2(r)$ changes its sign too. We now solve the differential equation.

The transformation to a new coordinate $\rho = 2i\omega r$ brings the differential equation into the form

$$\partial_\rho^2 \psi + \frac{2}{\rho} \partial_\rho \psi + \left(-\frac{1}{4} + \frac{n}{\rho} - \frac{s(s+1)}{\rho^2}\right) \psi = 0,$$

where $n = -i c_1/(2\omega)$ and $-s(s+1) = c_2$. The Ansatz $\psi(\rho) = (i\rho)^s e^{-\frac{\rho}{2}} f(\rho)$ yields the Kummer equation for f

$$\rho \partial_\rho^2 f + (2s + 2 - \rho) \partial_\rho f + (n - s - 1) f = 0,$$

so that the wave function turns out to be

$$\begin{aligned}
\psi(r) &= (2\omega r)^s e^{-i\omega r} \times \\
&\left[C_1 F(1 + s - n, 2s + 2, 2i\omega r) + C_2 (2i\omega r)^{-(1+2s)} F(-s - n, -2s, 2i\omega r) \right],
\end{aligned} \tag{26}$$

where we have chosen $s \geq -\frac{1}{2}$. The functions F are the confluent hypergeometric functions. The second term in the square brackets of equation (26) is singular at $r = 0$. If we require $\psi(r)$ to be regular at the origin, C_2 has to be zero.

The solutions are illustrated in **figure 2a** and **figure 2b**. In **figure 2a** the wave functions are plotted for $l = 0$ and $\omega = 1$. The pairs of parameter

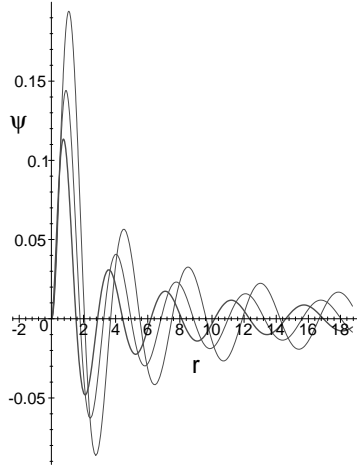


figure 2a: Wave functions for $\alpha_3 = \alpha_4 = 0$.

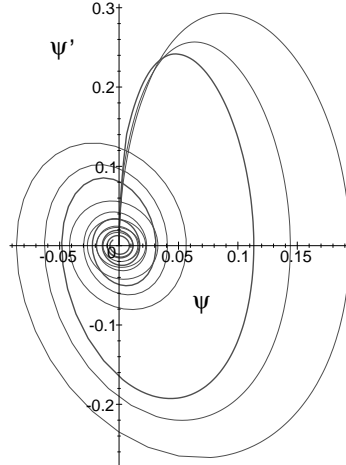


figure 2b: Phase space diagram for $\alpha_3 = \alpha_4 = 0$.

values $(\alpha_1, \alpha_2) = (11.0, -9.0), (12.0, -8.0), (13.0, -7.0)$ are indicated by lines of increasing thickness. In **figure 2b** we see the phase space diagram for the wavefunctions with parameter values as indicated above.

If α_3 and α_4 are not zero we have to integrate the differential equation (22) numerically. The wave functions and the phase space diagrams are shown in **figure 3a** and **figure 3b**.

Again we have chosen l to be equal to zero and $\omega = 1.0$. The lines of increasing thickness correspond to the following triples of parameter values $(\alpha_1, \alpha_2, \alpha_4) = (4.0, -1.0, -4.0), (3.0, -1.0, -3.0), (2.0, -1.0, 2.0)$ (α_3 is determined by equation (3)).

In **figure 4a, 4b, 5a** and **5b** we show how the shape of the wave function and the phase space diagrams change with increasing or decreasing value of ω . In these cases the parameters are $\alpha_1 = 1.0, \alpha_2 = -1.0$ and $\alpha_4 = -1.0$.

Some information about the scattering can be obtained analytically in terms of a WKB approximation [17]. Applying the transformation $\psi(r) = \theta(r)/r$ to (22), we obtain a differential equation for $\theta(r)$

$$\partial_r^2 \theta - Q(r) \theta = 0, \quad (27)$$

with

$$Q(r) = \omega^2 Q_0(r) + Q_2(r) = -\omega^2 F^2(r) + \frac{l(l+1)}{r^2}.$$

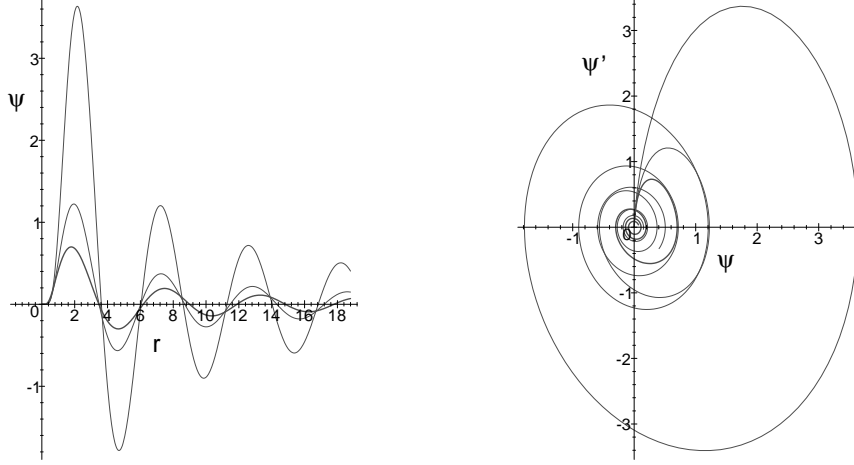


figure 3a: Wave functions for $\alpha_3, \alpha_4 \neq 0$. **figure 3b:** Phase space diagram for $\alpha_3, \alpha_4 \neq 0$.

If we set $\epsilon = 1/\omega$ and substitute the WKB ansatz

$$\theta(r) = \exp\left(\frac{1}{\epsilon} \left[\sum_{n=0}^{\infty} \epsilon^n S_n(r) \right]\right)$$

into equation (27) differential equations for the S_n 's are obtained. If the series is truncated after S_1 what results is called the physical optics approximation. The corresponding differential equations are

$$S_0'^2 = Q_0, \quad (28a)$$

$$2 S_0' S_1' + S_0'' = 0, \quad (28b)$$

$$2 S_0' S_2' + S_1'' + S_1'^2 = Q_2. \quad (28c)$$

The solutions are

$$S_0^\pm(r) = \pm \int_{r_h}^r \sqrt{Q_0(t)} dt, \quad (29a)$$

$$S_1(r) = -\frac{1}{4} \ln |Q_0(r)|, \quad (29b)$$

$$S_2(r) = \pm \int_{r_h}^r \left(\frac{Q_0''}{8Q_0^{\frac{3}{2}}} - \frac{5}{32} \frac{Q_0'^2}{Q_0^{\frac{5}{2}}} \right) dt, \quad \text{for } l = 0. \quad (29c)$$

Therefore the physical optics approximation is

$$\theta(r) = \frac{1}{\sqrt[4]{|Q_0(r)|}} \left[C_1 e^{\frac{1}{\epsilon} \int_{r_h}^r \sqrt{Q_0(t)} dt} + C_2 e^{-\frac{1}{\epsilon} \int_{r_h}^r \sqrt{Q_0(t)} dt} \right].$$

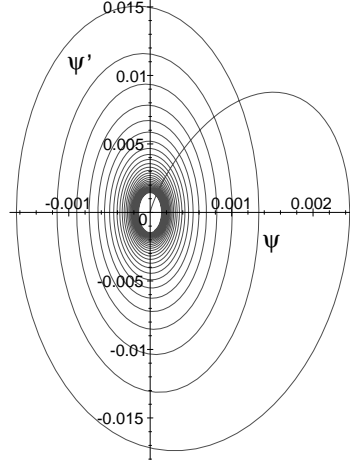
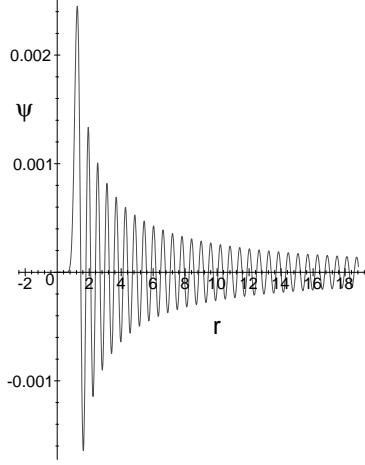


figure 4a: Wave function for $\omega = 10$.

figure 4b: Phase space diagram for $\omega = 10$.

It should be noted that the angular momentum component of the potential does not contribute to the physical optics approximation.

At $r = r_h$ the potential $Q_0(r)$ vanishes and the WKB approximation is not valid. Therefore we need to split the interval $[0, \infty)$ into three regions, a region I near $r = 0$, a region II near $r = r_h$ and a region III far outside, and they need to be investigated separately.

For $r < r_h$ the potential $Q_0(r)$ is positive and in addition we require $\psi(0)$ not to blow up exponentially. Consequently the wave function $\psi_I(r)$ in this region is given by

$$\psi_I(r) = \frac{C_1}{r \sqrt[4]{|Q_0(r)|}} e^{\frac{1}{\epsilon} \int_{r_h}^r \sqrt{Q_0(t)} dt} \quad \text{for } r < r_h.$$

As mentioned above the WKB approximation does not hold near $r = r_h$. However the potential near r_h can be approximated by a linear function with negative slope so that equation (27) in region II becomes approximately

$$\theta'' = \frac{a}{\epsilon^2} (r - r_h) \theta(r), \quad \text{where } a = Q'_0(r_h) < 0.$$

The solution of this approximate equation is

$$\psi_{II}(r) = \frac{1}{r} \left\{ C_a \text{Ai} \left[\epsilon^{-\frac{2}{3}} \sqrt[3]{-a} (r_h - r) \right] + C_b \text{Bi} \left[\epsilon^{-\frac{2}{3}} \sqrt[3]{-a} (r_h - r) \right] \right\}.$$

In region III $Q_0(r)$ is negative, so that $S_0(r)$ is pure imaginary and the wave function $\psi_{III}(r)$ can be written as

$$\psi_{III}(r) = \frac{1}{r \sqrt[4]{|Q_0(r)|}} \left\{ C_o e^{\frac{i}{\epsilon} \int_{r_h}^r \sqrt{|Q_0(t)|} dt} + C_i e^{-\frac{i}{\epsilon} \int_{r_h}^r \sqrt{|Q_0(t)|} dt} \right\}.$$

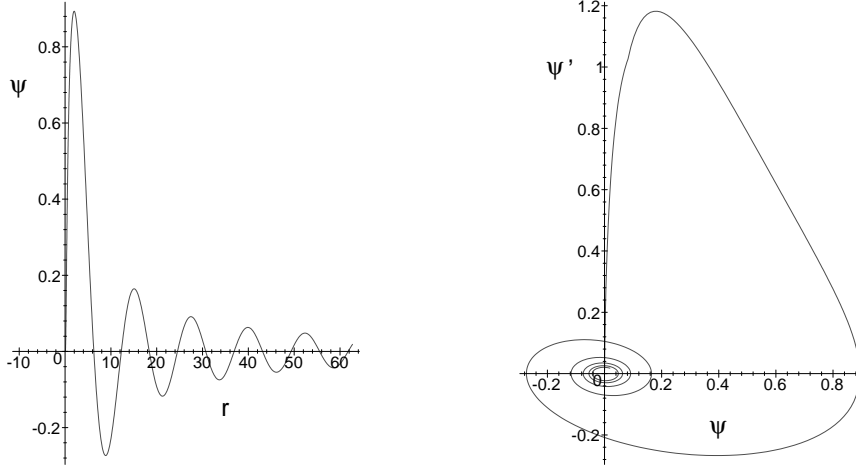


figure 5a: Wave function for $\omega = 0.5$.

figure 5b: Phase space diagram for $\omega = 0.5$.

We now try to patch these approximations together to obtain a solution on $[0, \infty)$. The matching procedure is done by estimating the range of validity of the solution in each region. In order that the WKB approximation be valid on an interval it is necessary that

$$\frac{S_0}{\epsilon} \gg S_1 \gg \epsilon S_2 \gg \dots \gg \epsilon_{n-1} S_n(x) \quad \text{for} \quad \epsilon \rightarrow 0. \quad (30)$$

We shall come back to this point in section 6.

In the overlapping regions we take into account the asymptotic behaviour of the respective solutions.

To match the functions $\psi_I(r)$ and $\psi_{II}(r)$ the asymptotic behaviour of the wave functions have to agree. For large positive arguments the Airy functions behave like

$$\text{Ai}(t) \sim \frac{1}{2\sqrt{\pi}} t^{-\frac{1}{4}} e^{-\frac{2}{3}t^{\frac{3}{2}}}, \quad \text{Bi}(t) \sim \frac{1}{\sqrt{\pi}} t^{-\frac{1}{4}} e^{\frac{2}{3}t^{\frac{3}{2}}}.$$

This shows that $C_b = 0$ and $C_a = \frac{2\sqrt{\pi}}{(-a\epsilon)^{\frac{1}{6}}} C_1$. We now fit the wave function in region II to region III. For large negative arguments the Airy function Ai behaves like

$$\text{Ai}\left(\epsilon^{-\frac{2}{3}} \sqrt{-a} (r_h - r)\right) \sim \frac{\epsilon^{\frac{1}{6}}}{\sqrt{\pi}} \frac{\sin\left(\frac{2}{3\epsilon} \sqrt{-a} (r - r_h)^{\frac{3}{2}} + \frac{\pi}{4}\right)}{(-a)^{\frac{1}{12}} (r - r_h)^{\frac{1}{4}}},$$

that is

$$\psi_{II}(r) \sim C_a \frac{\epsilon^{\frac{1}{6}}}{\sqrt{\pi} r} \frac{\sin\left(\frac{2}{3\epsilon} \sqrt{-a} (r - r_h)^{\frac{3}{2}} + \frac{\pi}{4}\right)}{(-a)^{\frac{1}{12}} (r - r_h)^{\frac{1}{4}}}.$$

In the overlapping region $\psi_{III}(r)$ is approximated by

$$\psi_{III}(r) \sim \frac{1}{r \sqrt[4]{-a} \sqrt[4]{r-r_h}} \left[C_o e^{\frac{2}{3\epsilon} i \sqrt{-a} (r-r_h)^{\frac{3}{2}}} + C_i e^{-\frac{2}{3\epsilon} i \sqrt{-a} (r-r_h)^{\frac{3}{2}}} \right]$$

The matching determines C_o and C_i via

$$\frac{C_a (-a\epsilon)^{\frac{1}{6}}}{\sqrt{\pi}} \sin\left(x + \frac{\pi}{4}\right) = C_o e^{ix} + C_i e^{-ix},$$

with $x = \frac{2}{3\epsilon} \sqrt{-a} (r - r_h)^{\frac{3}{2}}$. It follows that

$$C_o = C_a \frac{(-a\epsilon)^{\frac{1}{6}}}{2i \sqrt{\pi}} e^{\frac{1}{4} i \pi}, \quad C_i = -C_a \frac{(-a\epsilon)^{\frac{1}{6}}}{2i \sqrt{\pi}} e^{-\frac{1}{4} i \pi}$$

and therefore

$$\psi_{III}(r) = C_a \frac{(-a\epsilon)^{\frac{1}{6}}}{\sqrt{\pi}} \frac{1}{r \sqrt[4]{|Q_0(r)|}} \sin\left(\frac{1}{\epsilon} \int_{r_h}^r \sqrt{|Q_0(r)|} dt + \frac{\pi}{4}\right).$$

Thus we have obtained the approximations ($\epsilon = \frac{1}{\omega}$):

$$\psi_I(r) = C_a \frac{(-a\epsilon)^{\frac{1}{6}}}{2\sqrt{\pi}} \frac{1}{r \sqrt[4]{|Q_0(r)|}} e^{\frac{1}{\epsilon} \int_{r_h}^r \sqrt{|Q_0(t)|} dt}, \quad (31a)$$

$$\psi_{II}(r) = C_a \frac{\text{Ai}\left(\epsilon^{-\frac{2}{3}} \sqrt[3]{-a} (r_h - r)\right)}{r}, \quad (31b)$$

$$\psi_{III}(r) = C_a \frac{(-a\epsilon)^{\frac{1}{6}}}{\sqrt{\pi}} \frac{1}{r \sqrt[4]{|Q_0(r)|}} \sin\left(\frac{1}{\epsilon} \int_{r_h}^r \sqrt{|Q_0(r)|} dt + \frac{\pi}{4}\right). \quad (31c)$$

6 Discussion

A comparison of the numerical solution and the physical optics approximation is given in **figure 6a** and **figure 6b**.

Figure 6a shows the numerical and the WKB solution for the parameter values $l = 0.0, \omega = 1.0, \alpha_1 = 1.0, \alpha_2 = -1.0$ and $\alpha_4 = -1.0$. **Figure 6b** is a plot of the numerical solution and the WKB solution for a larger value, $\omega = 2.0$. The normalizations of the solutions are such that the numerical and the approximate solution agree at a position r_0 , with $0 < r_0 < r_h$. As is to be expected, the approximation improves as ω increases.

We investigated the range of validity for the approximate solutions numerically. For the physical optics approximation to be valid the conditions (30) have to hold up to the term S_2 . The numerical results are illustrated in **figure 7a** and **figure 7b** for $\omega = 1.0$ and $\omega = 2.0$, respectively. As a rough estimate for the matching intervals we find the following results: If $\omega = 1.0$, matching of $\psi_I(r)$ and $\psi_{II}(r)$ and $\psi_{II}(r)$ and $\psi_{III}(r)$ seems to be possible in the intervals

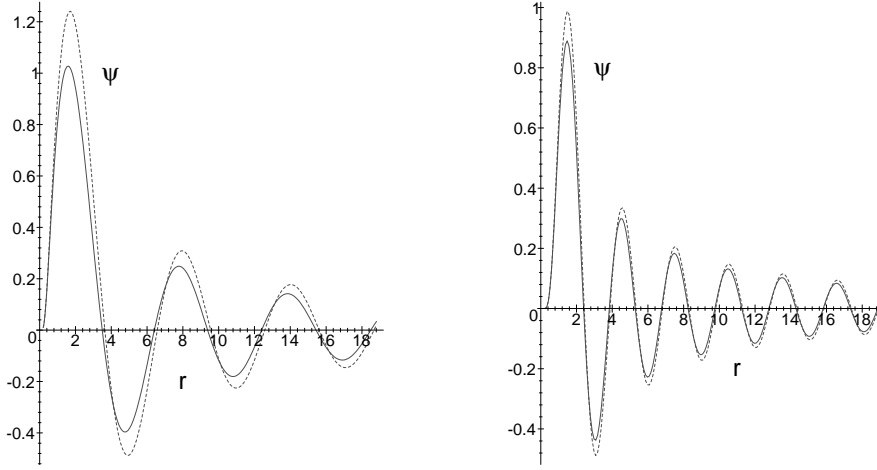


figure 6a: Numerical (dashed line) and **figure 6b:** Numerical (dashed line) and WKB solution (solid line) for $\omega = 1.0$ WKB solution (solid line) for $\omega = 2.0$

$[r_h - \text{tol}, 0.8]$ and $[1.4, r_h + \text{tol}]$. Here tol is calculated so that the argument of the Airy function remains small, i.e. $\text{tol} = \sqrt[3]{-\frac{\epsilon^2}{a}}$. For $\omega = 2.0$ the corresponding intervals are $[r_h - \text{tol}, 0.75]$ and $[1.4, r_h + \text{tol}]$.

At $r = \infty$ the WKB approximation predicts a phase shift of $\delta = \frac{\pi}{2}$ between the ingoing and the outgoing mode. For large r the ‘‘WKB phase shift’’ $\delta_{WKB}(r)$ is calculated for the global WKB approximation and extracted from the data for the numerical solution. The phase shift at $r = 20.0$ for the $\omega = 1.0$ data is $\delta_{WKB} = 89.54^\circ$. The numerically obtained phase shift δ_{num} is $\delta_{num} = 68.32^\circ$. For $\omega = 2.0$ the WKB phase shift is equal to $\delta_{WKB} = 89.82^\circ$ and the numerical value is $\delta_{num} = 78.71^\circ$. Furthermore the WKB approximation suggests that the amplitudes of the ingoing and the outgoing modes decay as $\sqrt{|C_o|^2 + |C_i|^2}/(2r)$. The modulus of the amplitudes of the ingoing and the outgoing mode are equal $|C_o| = |C_i|$, that is the reflection coefficient is equal to one.

For the special repulson data $\alpha_3 = \alpha_4 = 0$ we can gain some insight into the scattering behaviour even for regions of the parameters where the physical optics approximation breaks down (i.e. for small ω and $l \neq 0$).

To investigate the asymptotic behaviour of the wave function (26) we use the expansion of the Kummer function for large r (see [18]). Truncation of the asymptotic series after the first term yields

$$\begin{aligned} \psi(r) &\sim (2\omega r)^s \left[e^{-i\omega r} \frac{(-2i\omega r)^{n-s-1}}{\Gamma(n+s+1)} + e^{i\omega r} \frac{(2i\omega r)^{-n-s-1}}{\Gamma(-n+s+1)} \right] \\ &\sim \frac{1}{r} \sin \left(\omega r + 2M\omega \ln 2\omega r - \frac{\pi}{2}s + \arg[\Gamma(1+s-2iM\omega)] \right). \end{aligned}$$

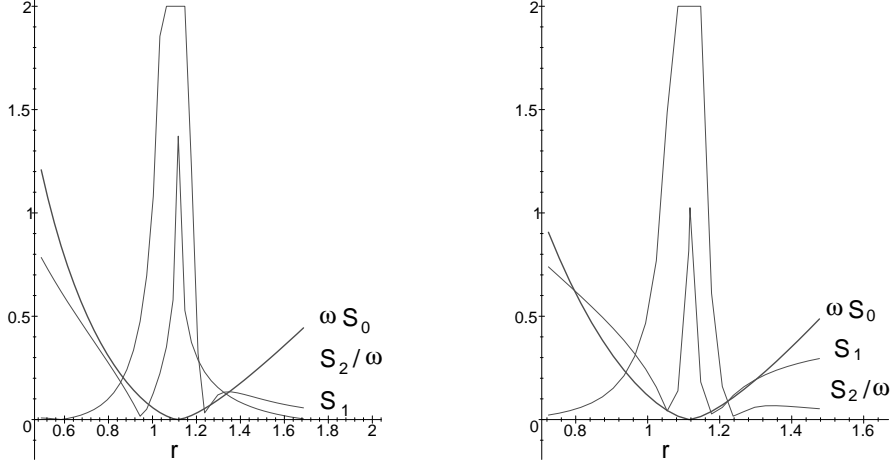


figure 7a: Comparison of $\omega S_0, S_1$ and **figure 7b:** Comparison of $\omega S_0, S_1$ and S_2/ω for $\omega = 1.0$

Therefore the modulus of the amplitudes of the ingoing and the outgoing mode are still equal. But we find a phase shift of $\delta = -\frac{\pi}{2}s + \arg[\Gamma(1 + s - 2iM\omega)]$. In particular the phase shift is no longer independent of the physical data of the repulson. In order to get a feeling where the physical optics approximation “leaks” we apply it to the repulson with $\alpha_3 = \alpha_4 = 0$. The potential is in this case given by

$$Q_0(r) = -1 - \frac{4M}{r} + \frac{s(s+1)}{r^2}. \quad (32)$$

Substitution of an asymptotic expansion of $S_0^+(r) \sim r + 2M \ln r$ into (31c) yields

$$\psi_{III}(r) = \frac{1}{r} \sin\left(\omega r + 2M\omega \ln r + \frac{\pi}{4}\right). \quad (33)$$

The physical optics approximation predicts total reflection and a phase shift of $\frac{\pi}{2}$ independent of the repulson data. The phase shift is constant, i.e. it contains the zeroth order contribution only. Let us expand the phase shift of the analytical solution in powers of ω .

$$\begin{aligned} \delta &= -\frac{\pi}{2}s + \arg \Gamma(1 + s - 2iM\omega) \sim \frac{\pi}{4} + \frac{\pi}{2}\omega + \arg \Gamma(1 + s - 2iM\omega) \\ &\sim \frac{\pi}{4} + \omega(2M+1) + \omega^2 |1 - 2Mi| (-\sin 4M - 2M \cos M), \end{aligned}$$

where we approximated s by $s \sim -\frac{1}{2} + \omega$. That is the WKB approximation predicts the zeroth order term in the phase shift. However, the exact solution also contains first and second order contributions. This shows that although the physical optics approximation represents the functional behaviour nicely it does not approximate the numerical value of the phase shift to a high precision.

This agrees with the observations we made in the case α_3 and α_4 unequal to zero.

To summarize: we studied the behaviour of a scalar test-particle in the metric background of a repulson. It has a curvature singularity at a finite distance r_h and a coordinate singularity at $r = 0$. Although the metric changes at r_h from a Lorentzian one to one with a Euclidean signature there is nothing peculiar about the position r_h of the curvature singularity at the quantum level. In contrary, near the coordinate singularity at the origin the particle feels a potential barrier and gets reflected. In terms of a semi-classical approximation, i.e. high frequency of the ingoing particle, there is an equal incoming and outgoing flux, i.e. the scattering matrix is unitary. The particle is phase shifted by $\frac{\pi}{2}$. The numerical data indicate – as expected – that the WKB approximation does not suit very well for incoming particles with low frequency. For special values of the repulson data ($\alpha_3 = \alpha_4 = 0$) we succeeded in working out the asymptotic behaviour analytically. We again find total reflection but the phase shift for a low frequency incoming particle depends on the physical data of the repulson. In particular the scattering behaviour of the scalar test-particle at the repulson supports the conjectures that gravitational singularities might be smeared out quantum mechanically.

There are other indications that credit should be given to these naked singularities. First of all – as they are repulsive in nature – they are not a complete disaster from the cosmic censorship point of view. The singularity is not shielded by a horizon but instead by an effective repulsive barrier at which scalar test-particles bounce off. In addition they very often correspond to solutions of a higher dimensional Kaluza-Klein like theory which usually have different properties. Singularities are resolved or naked singularities correspond to black holes in higher dimensions. It might be possible to establish some relations between these solutions and their properties. Unfortunately – although the repulsions can be associated to solutions of 5 dimensional low energy effective string theory – they do not correspond to black holes. At least not, if we take the definition of a black hole seriously. They correspond to extremal dilatonic configurations which represent space-times with timelike singularities [21, 20, 19].

We think it would be very interesting to study non-extremal repulson configurations to which one can associate black holes and in the sequel entropy, temperature and so far. Even more interesting would be to investigate the behaviour of a wave packet travelling towards the repulsive barrier. The wave packet would serve as a model of a test-string which consists of an infinite number of modes. But for that it is necessary to treat the partial differential equation (19) in an appropriate manner, which we leave for further investigations.

Acknowledgment

One of the authors (H. R. H) is indebted to W. Gleißner and S. Theisen for valuable discussions and for reading parts of the manuskript. She also likes to thank G. Gibbons for some enlightening remarks on black holes.

The work has been supported in part by the UK Particle Physics and Astronomy Research Council and by the Deutsche Forschungsgemeinschaft (DFG).

References

- [1] Lüst D.: String vacua with N=2 supersymmetry in four dimensions, [hep-th/9803072](#), talk given at the 5th International Conference on Supersymmetries in Physics (SUSY 97), Philadelphia, PA, 27–31 May 1997.
Youm D.: Black holes and solitons in string theory, [hep-th/9710046](#).
- [2] Gibbons G. W., Horowitz G. T., Townsend P. K.: Higher-dimensional resolution of dilatonic black hole singularities, *Class. Quant. Grav.* **12**, 297–318 (1995).
- [3] Bekenstein J.: Black holes and entropy, *Phys. Rev.* **D7**, 2333–2346 (1973).
Hawking S.: Particle creation by black holes, *Comm. Math. Phys.* **43**, 199–220 (1975).
- [4] Strominger A.: Massless black holes and conifolds in string theory, *Nucl. Phys.* **B451**, 96–108 (1995).
Behrndt K.: About a class of exact string backgrounds, *Nucl. Phys.* **B455**, 188–210 (1995).
Cvetič M., Youm D.: Singular BPS saturated and enhanced symmetries of four-dimensional N=4 supersymmetric string vacua, *Phys. Lett.* **B359**, 87–92 (1995).
Hull C. M.: Duality, enhanced symmetry and massless black holes, Proceedings of Strings ‘95, World Scientific, 1996.
Cvetič M., Tseytlin A. A.: General class of BPS saturated dyonic black holes as exact superstring solutions, *Phys. Lett.* **B366**, 95–103 (1996).
Chan K.-L., Cvetič M.: Massless BPS saturated states on the two torus moduli subspace of heterotic string, *Phys. Lett.* **B375**, 98–102 (1996).
Ortin T.: Massless black holes as diholes and quadruholes, *Phys. Rev. Lett.* **76**, 3890–3893 (1996).
Behrndt K., Lüst D., Sabra W. A.: Moving moduli, Calabi-Yau phase transitions and massless BPS configurations in type II superstrings, *Phys. Lett.* **B418**, 303–311 (1998).
Cvetič M., Hull C. M.: Wrapped branes and supersymmetry, *Nucl. Phys.* **B519**, 141–158 (1998).

- [5] Gaida I.: Gauge symmetry enhancement and N=2 supersymmetric quantum black holes in heterotic string vacua, *Nucl. Phys.* **B514**, 227–241 (1998).
- [6] Kallosh R., Linde A.: Exact supersymmetric massive and massless white holes, *Phys. Rev.* **D52**, 7137–7145 (1995).
- [7] Ferrara S., Kallosh R., Strominger A.: N=2 extremal black holes, *Phys. Rev.* **D52**, 5412–5416 (1995).
- [8] Behrndt K., Lüst D., Sabra W. A.: Stationary solutions of N=2 supergravity, *Nucl. Phys.* **B510**, 264–288 (1998).
- [9] Gaida I.: Quantum probes of repulsive singularities in N=2 supergravity, *Class. Quant. Grav.* **15**, 2261–2269 (1998).
- [10] Scherk J.: Antigravity: A crazy idea?, *Phys. Lett.* **B88**, 265–267 (1979).
Bellucci S.: “1260: Phenomenology of antigravity in N=2,8 supergravity”, Talk presented at the International Conference on High Energy Physics, Jerusalem, Israel, 19-26. Aug. 1997, and reference therein.
- [11] Reissner H.: *Ann. Phys.* **50**, 106 (1916).
Weyl H.: *Sitz. Ber. Preuss. Akad. Wiss.* **465**, (1918).
- [12] de Wit B., Lauwers P. G., Van Proeyen A.: Lagrangians of N=2 supergravity–matter systems, *Nucl. Phys.* **B255**, 569–608 (1985).
de Wit B., Vanderseypen F., Van Proeyen A.: Symmetry structure of special geometries, *Nucl. Phys.* **B400**, 463–524 (1993).
- [13] Strominger A.: Special geometry, *Comm. Math. Phys.* **133**, 163–180 (1990).
- [14] Maldacena J., Strominger A., Witten E.: Black hole entropy in M-theory, *J. High Energy Phys.* **12**, 002 (1997).
- [15] Gaida I.: N=2 supersymmetric quantum black holes in five dimensional heterotic string vacua, *Phys. Lett.* **B429**, 297–303 (1998).
- [16] Landau L. D., Lifshitz E. M.: *The classical theory of fields*, Pergamon Press (1975).
- [17] Bender C. M., Orszag S. A.: *Advanced mathematical methods for scientists and engineers*, McGraw–Hill (1978).
- [18] Abramowitz M., Stegun I. A.: *Handbook of mathematical functions*, Dover Publications (1964).
- [19] Gibbons G. W., Wiltshire D. L.: Black Holes in Kaluza–Klein Theory, *Annals Phys.* **167**, 201–223 (1986).
- [20] Holzhey C., Wilczek F.: Black holes as elementary particles, *Nucl. Phys.* **B380**, 447–477 (1992).

- [21] Horowitz G. T., Marolf D.: Quantum probes of spacetime singularities, *Phys. Rev.* **D52**, 5670–5675 (1995).